Int J Solids Structures Vol 15, pp 479–491
© Pergamon Press Ltd 1979 Printed in Great Britain

0020-7683/79/0601-0479/$02 00/0

EFFECTS OF ENVIRONMENT, DAMPING AND SHEAR DEFORMATIONS ON FLUTTER OF LAMINATED COMPOSITE PANELS†

SAILENDRA N. CHATTERJEE
Materials Sciences Corporation, Blue Bell Office Campus, Blue Bell, PA 19422, U.S.A.

and

SATISH V. KULKARNI‡
Lawrence Livermore Laboratory, Livermore, CA 94550, U.S.A.

(*Received* 31 *May* 1978, *in revised form* 8 *November* 1978)

Abstract—Flutter type instability of laminated fiber composite panels is studied based on piston theory aerodynamics and a laminated plate theory which includes the effects of shear deformations. Structural damping is considered in terms of frequency-dependent complex moduli of constituents. Stiffness of the laminae and the laminates are obtained by the use of well known elastic solutions and the dynamic elastic-viscoelastic correspondence principle. A modal method of solution is employed for obtaining flutter boundaries of panels which are constrained to deform in a state of plane deformation, i.e. cylindrical bending. Numerical results are reported for some Graphite/Epoxy laminates which are representative of laminated panels used in aircraft structures. Use is made of the shift hypothesis and shift factors of the epoxy matrix to study effects of environmental factors like temperature and moisture content.

1. INTRODUCTION

Dynamic response of composite materials has been investigated in the past with the objective of assessing the influence of geometry and material variables upon the vibrational frequencies and dispersion characteristics in composite laminates[1–4]. These studies are an essential first step in assessing the response of a structure subjected to more complex transient and aerodynamic loads which are frequently experienced in aerospace structures. An important conclusion which can be drawn from these investigations is that the effects of material anisotropy can be important for the problem of flexure, where shear and flexural deformations may be of comparable order. In addition, since shear properties and damping characteristics are primarily matrix dependent, it appears that the combined effects of damping and shear deformations will play an important role in the dynamic response of composite materials.

The problem of damping in composite materials has been investigated both analytically[5–8] and experimentally[8–11]. It is also well known that environmental conditions like temperature and humidity have a strong influence on static and dynamic properties of composite materials[12–15]. However, combined effects of damping, shear deformation and environmental factors on dynamic response of composite structures have not been investigated in detail. The main objective of the present work is to obtain analytical estimates of these effects on panel flutter of fiber-reinforced epoxy matrix composites.

Considerable work has been done on the problem of panel flutter over the past two decades and the studies can be classified under various categories[16, 17] depending on structural and aerodynamic theories employed. Since it is not the intent of this study to investigate effects of geometric nonlinearities and appropriateness of various aerodynamic theories, linear structural theory and linear piston theory aerodynamics[18] are utilized here. Panel flutter usually occurs at Mach numbers greater than one and therefore, the quasistatic aerodynamic theory seems adequate for the problem under consideration. The structural theory employed is the laminated plate theory[1]. Use of linear theories reduces the problem to determination of flutter boundaries, i.e. the critical values of the dynamic pressure for incipient flutter at which sustained

†Present results were obtained in the course of research supported by AFOSR Contract No. F44620-76-C-0080 with Materials Sciences Corporation.

‡Formerly with: Materials Sciences Corporation, Blue Bell, PA 19422, U.S.A.

simple harmonic motions are possible. Therefore, constitutive relations of a laminated panel with linearly viscoelastic constituents can be expressed in terms of frequency dependent complex dynamic moduli or stiffnesses employed in forced vibration problems of dynamic viscoelasticity. As a consequence straightforward but attractive procedures based on elastic–viscoelastic correspondence principle can be utilized to calculate lamina and subsequently laminate dynamic moduli from constituent fiber and matrix properties. These procedures are well known and therefore only a brief outline of the approach is given in the next section.

Effects of aerodynamic as well as structural damping on flutter of isotropic panels have been studied in the past[19, 20]. The results show that although velocity dependent damping increases the critical dynamic pressure, structural damping incorporated in the form of viscoelastic complex moduli can frequently have a destabilizing effect. Several investigations on flutter of sandwich and orthotropic panels are reported in literature[21–23]. It has been observed that inclusion of shear flexibility and rotary inertia admits two additional degrees of freedom, namely, thickness shear and thickness twist modes. Failure to account for these modes can lead to significant overestimates of the flutter dynamic pressure values. Recently, some studies have been directed towards composite laminates[24, 25] which indicate ply orientations and anisotropy ratios strongly influence the dynamic instability of such panels. Results for the studies discussed above indicate that the problem under consideration is a complex one and is influenced by various other factors like panel geometry, boundary conditions, flow angle, prestress, etc. The emphasis in this study is on the composite material parameters and environmental conditions and hence, a simple panel configuration may be considered. The logical choice is the one corresponding to cylindrical bending deformation of a plate simply supported at two parallel edges and infinitely long in the direction parallel to these edges. Procedures for flutter analysis of such panels and iterative methods of solution are described in Section 3.

2. DYNAMIC MODULI OF LAMINATED PLATES

If the fiber and matrix complex moduli (storage and loss moduli) are known from experiments as a function of frequency and environmental conditions, it is a relatively straightforward task to obtain the lamina/laminate complex moduli by utilizing the dynamic viscoelastic correspondence principle. This principle states that "the effective complex moduli of a viscoelastic composite are obtained by replacing the phase elastic moduli by the phase complex moduli in the expressions for the effective elastic moduli of identical phase geometry"[5]. Closed form expressions of effective moduli of unidirectional fiber reinforced composites with elastic isotropic constituents based on different micromechanical models[5, 26, 27] are available in literature. It has been observed that properties calculated from such expressions can sometimes differ significantly from exact numerical solutions and experimental measurements for monofilament and "square array" composites[6]. However, for commonly used structural composites with random arrangement of fibers such expressions have been found to be adequate for elastic as well as viscoelastic constituents[8, 28]. In this study, use is made of the results based on the composite cylinder assemblage model[5, 26] with transversely isotropic constituents. The fibers are assumed to be distributed in a random fashion with the plane of isotropy perpendicular to the axis of the fibers. Exact expressions for four of the five independent elastic moduli and an upper bound estimate for the other modulus are utilized. It is an easy matter to obtain the required expressions in the case of transversely isotropic phases from the results in [5, 26] and therefore, they are not given here. It should be mentioned here that if complex moduli of unidirectional lamina materials are known, laminate complex moduli can be readily evaluated by the procedure described subsequently. However, complex moduli of fiber-reinforced composites over a wide range of frequencies, temperatures and moisture concentrations are not available in literature. The procedure described here provides a reasonable basis for obtaining analytical estimates of these moduli from known fiber and matrix properties. Other simple algebraic expressions for effective elastic moduli like those in [27] are equally well suited for utilization of the correspondence principle.

Constitutive relations and equations of motion of the laminate are obtained by the use of elastic laminated plate theory[1] and the correspondence principle is once again invoked. Similar procedures have been employed in the past to the analysis of laminated beams[11].

Extensional, bending and extension-bending coupling stiffnesses are obtained by the use of relationships between plate and lamina stiffnesses given in [1]. Stiffnesses relating shear forces to average shear strains are, however, calculated on the assumption of "constant shear stress" in the laminate[29] instead of the "constant strain" field employed in[1]. Shear correction factors associated with these stiffnesses are evaluated by matching cut-off frequencies of thickness shear waves of infinitely large wave length calculated from elasticity and laminated plate theories. It is shown in [30] that these factors are functions of stacking sequence and orientations of the plies in the laminate, as well as the ratio of the two principal shear moduli of each ply. Shear moduli in a viscoelastic problem are frequency-dependent complex quantities and therefore, according to the correspondence principle, the correction factors for such a case could be different from the elastic solution. It is known, however, that the correction factors for elastic laminates constructed with a sequential arrangement of plies approach the well-known solution for a homogeneous plate ($\pi^2/12$) as the number of layers is increased[30]. When the two shear moduli of each ply are close to one another, the correction factors are close to $\pi^2/12$ even with a relatively small number of layers. Therefore, use of the factors evaluated in the elastic case for all frequencies in the viscoelastic problem is not likely to introduce any significant inaccuracy in the analysis attempted here.

3. GOVERNING EQUATIONS AND METHOD OF SOLUTION

The laminated plate of thickness h with a prescribed temperature and moisture distribution across the thickness is referred to a Cartesian co-ordinate system with z-axis normal to plate surfaces. Since the panel is constrained to deform in cylindrical bending, the analysis variables are independent of the y co-ordinate. Following[1], displacements u, v, w in the x, y, and z directions are assumed in the form given below.

$$\begin{aligned} u &= u^0(x,t) + z\psi_x(x,t) \\ v &= v^0(x,t) + z\psi_y(x,t) \\ w &= w(x,t). \end{aligned} \tag{1}$$

Using the relationships in [1, 29] and the correspondence principle, the governing equations for panel flutter can be written as:

$$\begin{aligned} &\tilde{A}_{11}u^0_{,xx} + \tilde{A}_{16}v^0_{,xx} + \tilde{B}_{11}\psi_{x,xx} + \tilde{B}_{16}\psi_{y,xx} = Pu^0_{,tt} + R\psi_{x,tt} \\ &\tilde{A}_{16}u^0_{,xx} + \tilde{A}_{66}v^0_{,xx} + \tilde{B}_{16}\psi_{x,xx} + \tilde{B}_{66}\psi_{y,xx} = Pv^0_{,tt} + R\psi_{y,tt} \\ &\tilde{K}_{55}(\psi_{x,x} + w_{,xx}) + \tilde{K}_{45}\psi_{y,x} = \frac{2q}{\beta}\cos\Lambda w_{,x} + \rho_a c w_{,t} + N^0_{xx}w_{,xx} + Pw_{,tt} \\ &\tilde{B}_{11}u^0_{,xx} + \tilde{B}_{16}v^0_{,xx} + \tilde{D}_{11}\psi_{x,xx} + \tilde{D}_{16}\psi_{y,xx} - \tilde{K}_{55}(\psi_x + w_{,x}) - \tilde{K}_{45}\psi_y = Ru^0_{,tt} + I\psi_{x,tt} \\ &\tilde{B}_{16}u^0_{,xx} + \tilde{B}_{66}v^0_{,xx} + \tilde{D}_{16}\psi_{x,xx} + \tilde{D}_{66}\psi_{y,xx} - \tilde{K}_{45}(\psi_x + w_{,x}) - \tilde{K}_{44}\psi_y = Rv^0_{,tt} + I\psi_{y,tt} \end{aligned} \tag{2}$$

where

ρ_a = free stream air density,
c = free stream speed of sound,
q = dynamic pressure of the airstream,
β = compressibility factor = $\sqrt{(M^2-1)}$
M = Mach number
N^0_{xx} = panel prestress
Λ = flow angle
P, R, I = inertial terms = $\int_{-h/2}^{h/2} \rho(1, z, z^2)\,dz$.

$\tilde{A}_{ij}, \tilde{B}_{ij}, \tilde{D}_{ij}$ $(i,j = 1,2,6)$ are the complex, frequency-dependent extensional, coupling and bending stiffnesses of the laminate[1], and $\tilde{K}_{ij} = k'_{ij}\tilde{A}'_{ij}$; $i,j = 4,5$; $\tilde{A}'_{ij}$ being the complex frequency dependent shear stiffness calculated from "constant stress" assumption[29]. k'_{ij} are the corresponding shear correction factors.

The aerodynamic loading is obtained from the linear piston theory[18]. The piston theory gives a simple expression for the aerodynamic loading. The expression $2q/\beta \cos \Lambda w_{,x}$ is the aerodynamic pressure term, while the term $\rho_a c w_{,t}$ represents aerodynamic damping. It is also assumed that the prestress is unaffected by the displacements in the plate.

The boundary conditions at $x = 0, a$ for a simply supported panel in terms of displacements, stress resultants and derivatives of displacements are

$$\begin{aligned} w &= 0, \\ N_{xx} &= \tilde{A}_{11}u^0_{,x} + \tilde{A}_{16}v^0_{,x} + \tilde{B}_{11}\psi_{x,x} + \tilde{B}_{16}\psi_{y,x} = 0, \\ N_{xy} &= \tilde{A}_{16}u^0_{,x} + \tilde{A}_{66}v^0_{,x} + \tilde{B}_{16}\psi_{x,x} + \tilde{B}_{66}\psi_{y,x} = 0, \\ M_{xx} &= \tilde{B}_{11}u^0_{,x} + \tilde{B}_{16}v^0_{,x} + \tilde{D}_{11}\psi_{x,x} + \tilde{D}_{16}\psi_{y,x} = 0, \end{aligned} \tag{3}$$

and

$$M_{xy} = \tilde{B}_{16}u^0_{,x} + \tilde{B}_{66}v^0_{,x} + \tilde{D}_{16}\psi_{x,x} + \tilde{D}_{66}\psi_{y,x} = 0.$$

In what follows, the following nondimensional quantities will be utilized:

$$\begin{gathered} X, U_0, V_0, W = (x, u_0, v_0, w)/a \\ A_{ij}, B_{ij}, D_{ij}, K_{ij} = (a^2\tilde{A}_{ij}, a\tilde{B}_{ij}, \tilde{D}_{ij}, a^2\tilde{K}_{ij})/D_0 \\ \bar{P}, \bar{R}, \bar{I} = (a^4P, a^3R, a^2I)/D_0 \\ \bar{\lambda} = \frac{2a^3q \cos \Lambda}{\beta D_0}, \quad S = \frac{a^4\rho_a c}{D_0} \quad \text{and} \quad \bar{N}_{xx} = \frac{a^2N^0_{xx}}{D_0} \end{gathered} \tag{4}$$

and D_0 = real part of the bending stiffness $\tilde{D}_{11}$ corresponding to the first frequency in the chosen frequency range. The governing differential equations in terms of displacements U_0, V_0, W and rotations ψ_x, ψ_y are the same as eqn (2) with all the quantities replaced by their nondimensional counterparts in eqns (4). Following well known methods of solution, the displacement variables are expressed in the form given below.

$$\begin{aligned} W &= -e^{i\omega t}\sum_{n=1}^{\infty}\frac{a_n}{\alpha_n}\sin \alpha_n X \\ \psi_x + W_{,X} &= e^{i\omega t}\sum_{n=1}^{\infty} b_n \cos \alpha_n X \\ U^0 &= e^{i\omega t}\sum_{n=1}^{\infty} c_n \cos \alpha_n X \\ \psi_y &= e^{i\omega t}\sum_{n=1}^{\infty} d_n \cos \alpha_n X \end{aligned}$$

and

$$V^0 = e^{i\omega t}\sum_{n=1}^{\infty} e_n \cos \alpha_n X \tag{5}$$

where $\alpha_n = n\pi$. The boundary conditions (3) are identically satisfied. Use of the Galerkin procedure in conjunction with eqns (2) and (5) yields

$$\left\{[K_n] - \frac{\omega^2}{\alpha_n^2}[M_n]\right\}\{A_n\} + 4\bar{\lambda}\{L_n\} = 0; \quad n = 1, 2, \ldots, \infty \tag{6}$$

where

$$[K_n] = \begin{bmatrix} (D_{11} - \bar{N}_{xx}/\alpha_n^2 + iS\omega/\alpha_n^4) & D_{11} & B_{11} & D_{16} & B_{16} \\ D_{11} & (D_{11} + K_{55}/\alpha_n^2) & B_{11} & (D_{16} + K_{45}/\alpha_n^2) & B_{16} \\ B_{11} & B_{11} & A_{11} & B_{16} & A_{16} \\ D_{16} & (D_{16} + K_{45}/\alpha_n^2) & B_{16} & (D_{66} + K_{44}/\alpha_n^2) & B_{66} \\ B_{16} & B_{16} & A_{16} & B_{66} & A_{66} \end{bmatrix} \tag{7}$$

$$[M_n] = \begin{bmatrix} \bar{P}/\alpha_n^2 + \bar{I} & \bar{I} & \bar{R} & 0 & 0 \\ \bar{I} & \bar{I} & \bar{R} & 0 & 0 \\ \bar{R} & \bar{R} & \bar{P} & 0 & 0 \\ 0 & 0 & 0 & \bar{I} & \bar{R} \\ 0 & 0 & 0 & \bar{R} & \bar{P} \end{bmatrix} \tag{8}$$

$$[A_n] = \begin{bmatrix} a_n \\ b_n \\ c_n \\ d_n \\ e_n \end{bmatrix}, \text{ and } L_n = \begin{bmatrix} \sum_{\substack{m=1 \\ n-m=\text{odd}}}^{\infty} \dfrac{e_m}{(\alpha_n^2 - \alpha_m^2)\alpha_n^2} \\ 0 \\ 0 \\ 0 \\ 0 \end{bmatrix}. \tag{9}$$

On truncating each of the series in eqn (5) at $n \leq N$, eqn (6) yields a set of $5N$ homogeneous equations. For a non-trivial solution, the determinant of the coefficients a_n, b_n, c_n, d_n, e_n ($n = 1, 2, \ldots, N$) must equal zero. Standard eigenvalue routines cannot be used to calculate the eigenvalues ω_n^2 (for given $\bar{\lambda}$, the flutter parameter) since the elements of the matrix $[K_n]$ are frequency dependent. Hence, a trial and error procedure must be employed.

The panel behavior is characterized by the variation of $\omega_n = (\omega_R + i\omega_I)$ with $\bar{\lambda}$. It is clear that if the imaginary part, ω_I, is negative, a divergent motion ensues. If, on the other hand, ω_I is positive, the result is a damped harmonic motion. Thus, flutter is considered to occur for the lowest value of $\bar{\lambda}$ at which the imaginary part of the frequency changes sign, or in other words, vanishes. This condition corresponds to sustained simple harmonic motion and represents incipient flutter.

Given the frequency-dependent complex moduli of the constituents (fiber and matrix) at different temperatures and for various moisture concentrations, the lamina properties can be computed by the use of methods outlined in Section 2 giving due consideration to the actual temperature and moisture distribution in the laminate. Complex moduli of each lamina for various frequencies are calculated for the actual temperature and moisture content at the lamina location by the use of linear interpolation. One can then obtain the laminate properties and appropriate shear correction factors. At first, the eigenvalues for $\bar{\lambda} = 0$ corresponding to each n are determined. Attention is then restricted to frequencies less than or equal to the highest flexural frequency. This frequency range is then divided into several intervals. Average properties in each interval are then used to determine the points in each interval at which imaginary parts of eigenvalues change sign as $\bar{\lambda}$ is gradually increased. Properties at these points (corresponding to the real part of ω) are then used to recalculate the eigenvalue and the flutter parameter. This procedure is repeated to achieve the desired accuracy. Convergence of any trial and error procedure is strongly dependent on the starting point as well as the increments by which the unknown parameter is changed. The procedure used here has the same limitation and, therefore, in certain cases, it had to be repeated to obtain the results sought.

The analysis procedure outlined above yields complex eigenvalues except at the points of incipient flutter where the frequencies are real. Similar nonlinear eigenvalue problems involving complex frequencies arise in studies of damped free wave propagation in laminated viscoelastic composites[31]. It should be pointed out here that there is some difficulty in determination of frequency-dependent dynamic complex moduli of a material when the frequencies are complex. Representation of a viscoelastic body by a mechanical model, with a finite number of springs and dashpots, and use of curve fitting procedures yield expressions for complex modulus as a function of frequency, which can be used for real as well as complex frequencies. It is well known, however, that such procedures yield reasonable correlation with experimental data for commonly used materials only over a limited frequency range. On the other hand, measurements with forced vibration techniques can yield values of complex modulus as a function of real forcing frequency. However, in problems of viscoelastic vibration, which are usually of interest in practical applications, material damping is usually small. Under such circumstances, damped motions are characterized by complex frequencies with imaginary parts much smaller than the real ones. Moreover, the main interest in this study is the determination of flutter boundaries at which the imaginary parts are zero. Therefore, in this study, the complex moduli

are assumed to be functions of real part of the frequency and effect of non-zero imaginary parts is neglected. It should be mentioned that when the dynamic instability is severe in nature, magnitude of the imaginary parts of the eigenvalues increases rapidly with little increase in dynamic pressure and therefore, the results presented in the next section dealing with severity of instability should be considered as a first-order approximate solution. No refinements in these solutions are attempted here, since the small deformation theory used for the analysis is itself inadequate for studying the plate response after instability sets in.

4. RESULTS AND DISCUSSION

4.1 *Laminate geometries and constituent properties*

Procedures described in Sections 2 and 3 are employed to study effects of environmental conditions, damping, and shear deformation on flutter boundaries of the following laminates, each of thickness $h = 0.06$ in.:

(1) Laminate 1, $(0/90)_{2s}$, $a/h = 60$, $a = 3.6$ in.
(2) Laminate 2, $(0/90)_{2s}$, $a/h = 10$, $a = 0.6$ in.
(3) Laminate 3, $(\pm 45/0_2/90)_s$, $a/h = 40$, $a = 2.4$ in.
(4) Laminate 4, $(\pm 45/0_2/90)_s$, $a/h = 10$, $a = 0.6$ in.

The types and dimensions of the laminates are representative of those commonly used in practice. The 0° direction is assumed to coincide with the x-axis and all plies are made of the same material, which is a Thornel 300 type graphite fiber reinforced epoxy matrix composite with 50% volume fraction of fibers. The mass density of the material is $\rho = 0.00015$ lb-sec^2/in^4.

Graphitic materials do not show time-dependent response except at temperatures well above those considered in this study, and their properties are generally not influenced by moisture. Therefore, transversely isotropic T-300 fiber properties listed below are assumed to be real constants for all frequencies and environmental conditions:

Axial Young's modulus $E_A = 34 \times 10^6$ psi,
Transverse Young's modulus $E_T = 3 \times 10^6$ psi,
Axial Poisson's ratio $\nu_A = 0.26$
Transverse Poisson's ratio $\nu_T = 0.4$,
Axial shear modulus $G_A = 3.2 \times 10^6$ psi. (10)

ν_A refers to transverse strain due to imposed axial strain.

The epoxy matrix is isotropic and its properties are plotted against frequency in Fig. 1. To

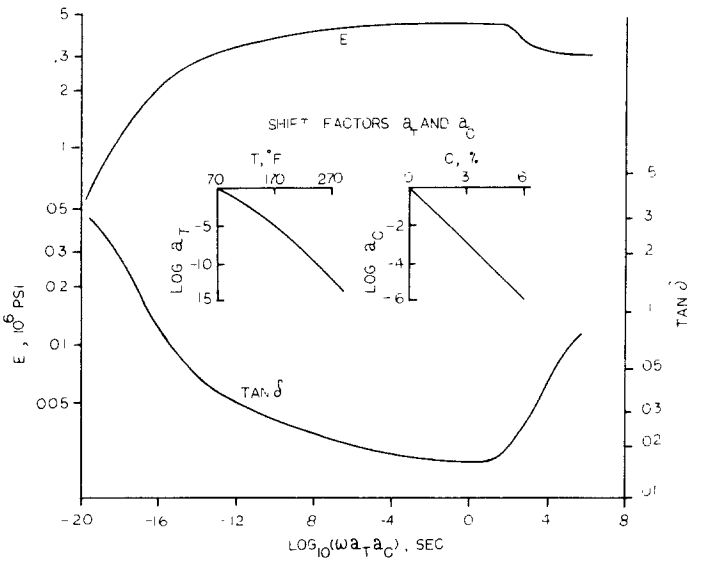

Fig. 1. Master curve and shift factors for dynamic properties of epoxy matrix, Ref. state $C = 0$, $T = 70$°F

calculate matrix properties at different temperatures and moisture concentrations, use is made of the well-known shift hypothesis[32, 33]. Assumed shift factors are also shown in the same figure. For frequencies in the range of 10–10^3 Hz, *in situ* storage modulus and loss tangents are assumed to be the same as those given in [7]. For low frequencies, these values are assumed to behave in a manner similar to those of an epoxy resin, as reported in [32] with due consideration to shifts. The bulk modulus of the matrix is usually a weak viscoelastic function[8] and therefore it is assumed to be 0.488×10^6 psi[7], which is real and constant for all temperature and moisture content.

4.2 *Dynamic moduli of laminates*

The real and imaginary parts of bending rigidity $\tilde{D}_{11}$ and shear stiffness $\tilde{A}'_{55}$ of the two types of laminates under consideration calculated by procedures described in Section 2 are plotted against frequency in Figs. 2 and 3. These stiffnesses have the greatest influence on laminate flutter characteristics. The solid lines in the figures represent the properties at reference state, i.e. the laminate is at room temperature (70°F) and is dry. The dotted lines are for prescribed moisture and temperature gradients as shown in the insert of Fig. 2. The temperatures at top and bottom surfaces are 250 and 70°F, respectively. Moisture concentration in the matrix materials on these surfaces are 2.57 and 0%. It can be seen that real parts of $\tilde{D}_{11}$ for both the laminates remain practically constant for all frequencies because of the presence of high-modulus elastic fibers. Frequency dependence and shift characteristics of the matrix storage modulus and loss tangent translate to the variations of imaginary parts of $\tilde{D}_{11}$ as well as real and imaginary parts of $\tilde{A}'_{55}$ with frequency and environmental conditions. For frequencies greater than 10^3 Hz, loss tangents for $\tilde{A}'_{55}$ and $\tilde{D}_{11}$ are reduced and storage moduli $\tilde{A}'^{R}_{55}$ are increased due to imposed moisture temperature gradients. As will be seen later, these changes have a significant influence on flutter characteristics of the laminates. It is clear that calculated laminate stiffnesses are strongly influenced by the master curve and shift characteristics of the matrix properties. For this reason, results obtained in this study are discussed and conclusions are drawn with due consideration to the laminate properties used. Effects of other types of input data can be estimated if the corresponding laminate stiffnesses are known.

Shear correction factors for the laminated plates estimated by matching the plate theory

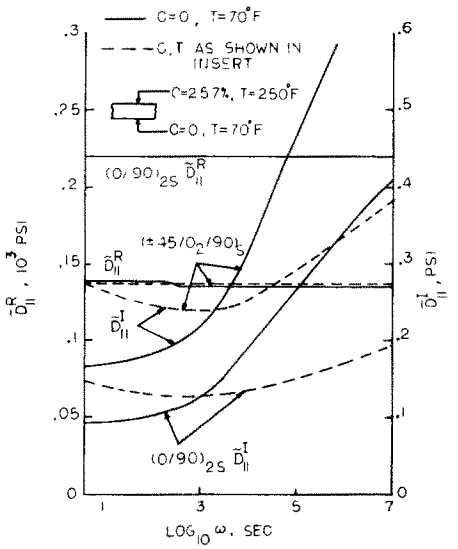

Fig. 2.

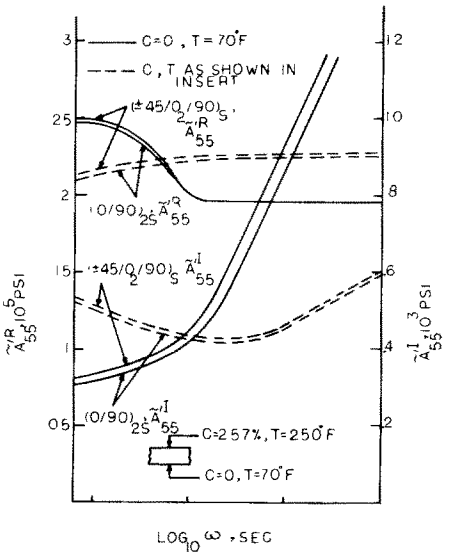

Fig. 3.

Fig. 2. Variation of real and imaginary parts of bending rigidity $\tilde{D}_{11}$ with frequency for $(0/90)_{2s}$ and $(\pm 45/0_2/90)_s$ laminates.

Fig. 3. Variation of real and imaginary parts of shear stiffness $\tilde{A}'_{55}$ with frequency for $(0/90)_{2s}$ and $(\pm 45/0_2/90)_s$ laminates.

solutions with those from elasticity theory[30] are listed below

Laminate	k'_{55}	k'_{44}	k''_{45}
$(0/90)_{2s}$	0.800	0.845	0.0
$(\pm 45/0_2/90)_s$	0.815	0.828	0.008

(11)

"Effective" shear stiffnesses are calculated as

$$\tilde{K}_{55} = k'_{55}\tilde{A}'_{55},\ \tilde{K}_{44} = k'_{44}\tilde{A}'_{44} \text{ and } \tilde{K}_{45} = k''_{45}\sqrt{(\tilde{K}_{55}\tilde{K}_{44})}. \tag{12}$$

As indicated in Section 2, the correction factors are assumed to remain constant irrespective of frequency and environmental conditions. The $(0/90)_{2s}$ laminates are orthotropic and therefore the "effective" coupling stiffness $\tilde{K}_{45}$ is zero. The $(\pm 45/0_2/90)_s$ laminates have a symmetric lay-up and therefore the coupling shear stiffness $\tilde{A}'_{45}$ is zero for symmetric moisture and temperature distribution and is small for the prescribed moisture, temperature gradients. However, presence of $\pm 45°$ plies introduces some amount of coupling between average strains in xz and yz planes and the "effective" coupling stiffness is evaluated by the relationship (12) given above. The factor k''_{45} is estimated by procedures described in [30].

4.3 *Nature of instabilities and effect of shear deformation*

Real and imaginary parts of $\bar{\omega} = \omega . Pa^4/D$ for various values of $\bar{\lambda} = 2a^3q/(\beta D_0)$ are plotted in Figs. 4–7 for the laminates 1–4, respectively. The values of critical flutter parameters are also listed in these figures. Five terms of the series representation ($N = 5$) were retained in all the calculations.

To assess convergence, flutter parameters were calculated for laminate 2 in the reference state by retaining up to nine terms of the series representation. No appreciable influence was noted in the lowest value of critical load. A change of the order of 6% could be observed in the value of the flutter parameter corresponding to the point of coalescence of fourth and fifth flexural modes. Changes of that order are expected due to the influence of neighboring higher modes. Similar influence was observed when environmental conditions (temperature and moisture) were altered. Therefore, accuracy of the results with five terms was considered sufficient for the purpose of the comparitive study reported herein. As indicated in Section 3, the frequency range of interest was divided into five parts and average stiffnesses in each part were used for obtaining the results except for the determination of the points of incipient flutter. In the latter case, calculations were repeated to obtain refined estimates by using the actual values of stiffnesses at the flutter frequency. Since input data for laminated plate stiffnesses do not fluctuate rapidly with change in frequency, use of average values yields

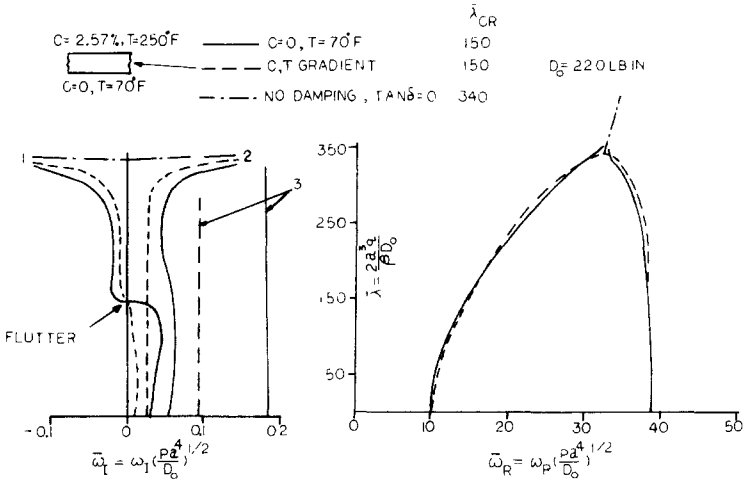

Fig. 4. Frequency spectrum for $(0/90)_{2s}$ cross-ply laminate 1, $a/h = 60$, $h = 0.06$ in.

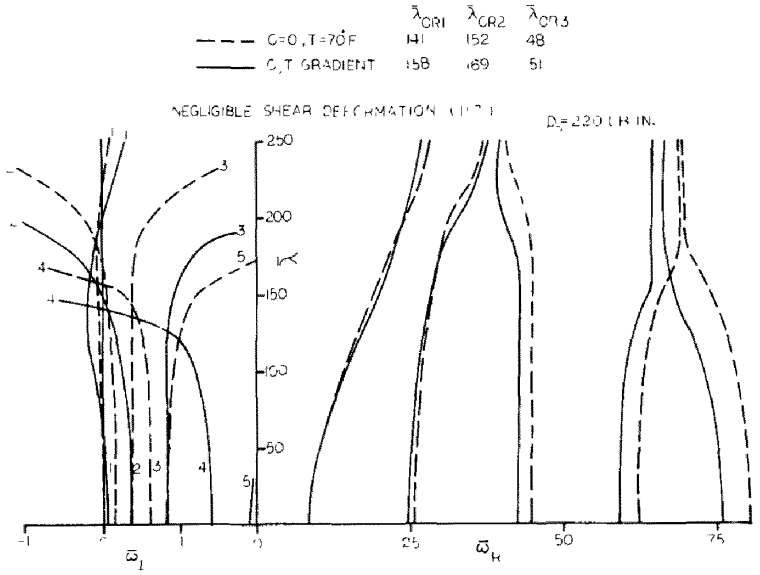

Fig. 5. Frequency spectrum for $(0/90)_{2s}$ cross-ply laminate 2, $a/h = 10$, $h = 0.06$ in.

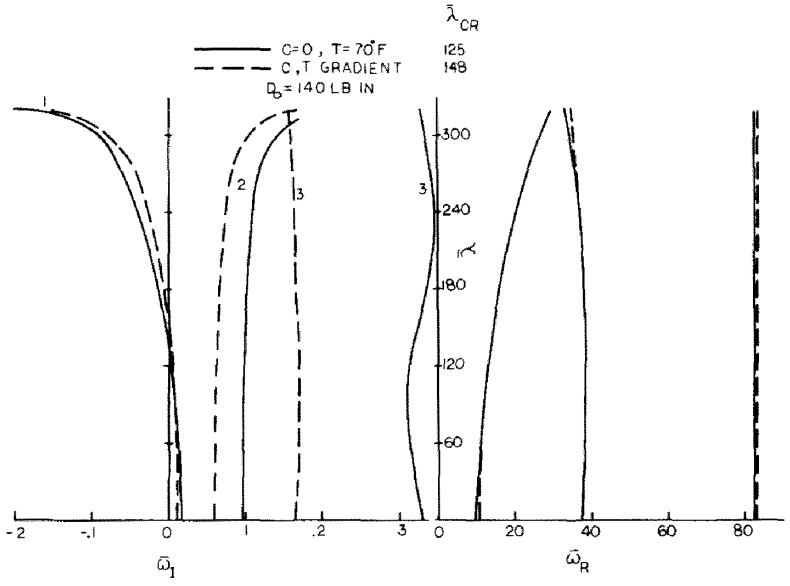

Fig. 6. Frequency spectrum for $(\pm 45/0_2/90)_s$ laminate 3, $a/h = 40$, $h = 0.06$ in.

reasonably accurate results. A total of twenty modes to include the effect of four displacement variables, W, $\psi_x + W_{,x}$, ψ_y and U_0 were considered in laminate 4, where bending-extension coupling effects due to unsymmetric moisture, temperature distribution should have the largest influence. No destabilizing effect was noticed. Extensional stiffnesses appear to be extremely high to have any influence on flutter characteristics. Therefore, fifteen modes were retained for laminate 3 and ten were retained for laminates 1 and 2, where there is no coupling between the shear deformations $\psi_x + W_{,x}$ and ψ_y.

For all four laminates under consideration, there exists a point of instability at which the real part of the frequency is close to that of free vibration in the first flexural mode and the value of $\bar{\lambda}_{cr}$ is much lower than what is expected in the absence of damping. However, the instability is not very severe in nature, i.e. absolute value of the imaginary part $\bar{\omega}_I$ of $\bar{\omega}$ does not increase rapidly with $\bar{\lambda}$ as $\bar{\lambda}$ is increased beyond the point of incipient flutter. It is worth noting that a similar type of "mild" instability called "single mode flutter" is often observed in experimental studies[17]. However, single mode flutter is usually due to loss of aerodynamic

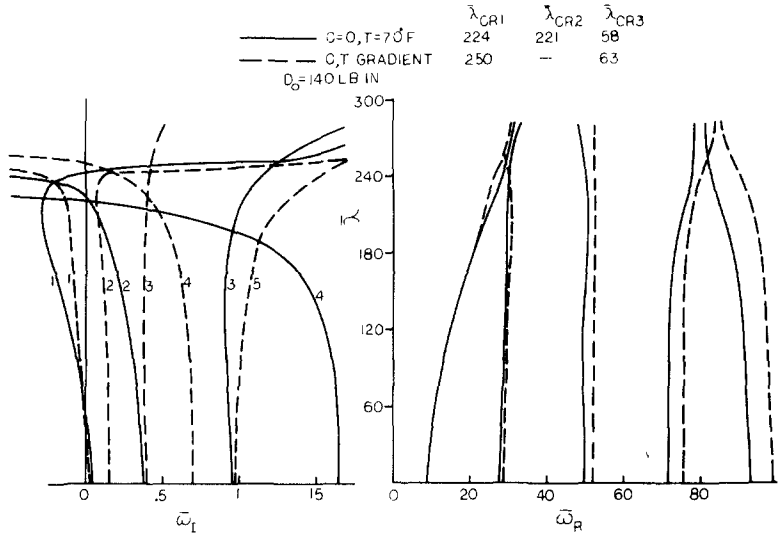

Fig. 7. Frequency spectrum for $(\pm 45/0_2/90)_s$ laminate 4, $a/h = 10$, $h = 0.06$ in.

damping at low supersonic Mach numbers where piston theory is inapplicable and no single mode flutter is possible for an isotropic plate without structural damping when piston theory is employed. In the results reported in Figs. 4–7, influence of aerodynamic damping is not included and therefore, the destabilizing effect noticed here appears to be due to a phase shift caused by structural damping.

For laminates 1 and 3 (Figs. 4 and 6) with large span-to-depth ratios, the shear deformation effects are small and $\bar{\omega}_I$ does not increase rapidly until $\bar{\lambda}$ is much higher than $\bar{\lambda}_{cr}$, the point of incipient flutter. Since the laminates are constrained to deform in cylindrical bending, their aerodynamic response should be similar to that of isotropic panels, when shear deformations are negligible. For this reason Fig. 4 looks very much like the result for an isotropic plate[18, 19]. For laminates 2 and 4 (Figs. 5 and 7), the points of "mild" instability are identified as $\bar{\lambda}_{cr3}$. For these laminates, shear deformations are comparatively large because the span-to-depth ratio is 10. There are two other values of $\bar{\lambda}_{cr}$ for laminates 2 and 4, i.e. $\bar{\lambda}_{cr1}$ and $\bar{\lambda}_{cr2}$, which are higher than $\bar{\lambda}_{cr3}$. Figure 5 clearly shows that for laminate 2, $\bar{\omega}_I$ becomes negative at $\bar{\lambda}_{cr3}$ and its magnitude then increases slowly with $\bar{\lambda}$. In fact, as $\bar{\lambda}$ is increased further, $|\bar{\omega}_I|$ decreases and $\bar{\omega}_I$ becomes positive again. Instabilities at $\bar{\lambda} = \bar{\lambda}_{cr1}$ and $\bar{\lambda}_{cr2}$ are much more severe. Shear deformation has a tremendous influence on the critical flutter parameter. By arbitrarily increasing the shear stiffness (multiplying the shear correction factor by 1000), the critical flutter parameter for laminate 5 is increased from 48 to 117 (see Fig. 5) and severe flutter occurs due to coalescence of modes 1 and 2.

In laminate 4 (Fig. 7), "mild" instability sets in at a very low value of $\bar{\lambda}$ as in the case of laminate 2, and as $\bar{\lambda}$ is increased significantly, $\bar{\omega}_I$ corresponding to mode 1 changes sign again from negative to positive, but $\bar{\omega}_I$ corresponding to mode 2 becomes negative and yields a severe instability. On the other hand, it appears that inclusion of moisture-temperature effects causes $\bar{\omega}_I$ corresponding to mode 1 to increase in magnitude causing a strong flutter instability. Near these points of severe instability, strong coupling exists between different modes. Although this behavior does not influence critical values of flutter parameters for "mild" or "severe" instabilities, it is an interesting phenomenon and should be investigated in detail in future studies.

4.4 *Environmental effects*

Moisture-temperature gradient does not appear to have much influence on the critical value of the flutter parameter for laminate 1, but increases the critical values for laminates 2–4. This beneficial effect, however, is not due to increased damping. Moisture-temperature gradient actually reduces the loss tangents of bending as well as shear stiffness of all laminates as is clear from the values of $\bar{\omega}_I$ at $\bar{\lambda} = 0$ and from Figs. 2 and 3. This is a consequence of the type of

master curve assumed (Fig. 1) and the shift hypothesis. Loss tangents for the epoxy matrix reduce with decreasing frequency up to $\omega \approx 10$. Increased temperature and moisture effects cause a shift towards the left in Fig. 1 by the shift hypothesis, which causes a reduction in loss tangent. For the same reason, the storage modulus increases due to moisture-temperature effects. The increase in shear stiffness is reflected in the increased values of $\bar{\lambda}_{cr}$ in laminates 2–4 where shear deformations have comparatively larger influence. Since $\bar{\lambda}_{cr}$ for laminate 1 is not strongly influenced by shear deformations, no increase is noticed in this case.

4.5 *Influence of material damping*

To investigate effects of material damping on critical values of $\bar{\lambda}_{cr}$, imaginary parts of matrix Young's modulus (for all frequencies) were multiplied by 0.0 (no damping), 0.25, 1.0 (base) and 2.5, and the calculations were repeated in each case for laminates 1 and 2. Corresponding damping levels are graded as 0, 1, 2 and 3 respectively. The real part of Young's modulus and the bulk modulus were maintained constant at all levels. Results are tabulated in Table 1.

Table 1. Effects of material damping levels on flutter parameter $\bar{\lambda}_{cr}$ for $(0/90)_{2s}$ laminates

Level of damping	Laminate 1, $a/h = 60$	Laminate 2, $a/h = 10$		
	$\bar{\lambda}_{cr}$	$\bar{\lambda}_{cr1}$	$\bar{\lambda}_{cr2}$	$\bar{\lambda}_{cr3}$
0, No damping	340	148	205	—
1	157	139	152	48
2, Base	150	141	152	48
3	150	152	155	48.5

For laminate 2, $\bar{\lambda}_{cr1}$, $\bar{\lambda}_{cr2}$ and $\bar{\lambda}_{cr3}$ appear to increase as damping level is increased from 1 to 3. For no damping, there does not appear to be any point of incipient flutter corresponding to $\bar{\lambda}_{cr3}$ for cases with damping. This point $\bar{\lambda}_{cr3}$ is, however, not a point of severe instability. For laminate 1, $\bar{\lambda}_{cr}$ sharply drops from a value of 340 for zero damping to 157, 150 and 150 for damping levels 1, 2 and 3, respectively. Similar strong destabilizing influences of small damping have been observed in other studies of dynamic instability[19, 34]. The reason for a higher value of $\bar{\lambda}_{cr}$ for level 1, as compared to those for levels 2 and 3, is not clear. This trend is different from that for laminate 2, which shows some increase in $\bar{\lambda}_{cr}$ as damping is increased from level 1 to 3. It should be noted, however, that the imaginary part of $\bar{\omega}$ sharply changes from negative to positive in the case of laminate 1 (see Fig. 4) as it passes through $\bar{\lambda}_{cr}$, and the properties used for calculations are obtained by linear interpolation from those given in a tabular form. In view of these facts, the small difference discussed above does not appear to be significant. It should be pointed out here that the drop in $\bar{\lambda}_{cr}$ due to introduction of small damping is significantly higher when shear deformation effects are small (a/h is large) as compared to the cases when such effects are dominant (a/h is small).

4.6 *Effects of various factors on severity of instability*

A simple way to assess the severity of flutter is to examine how the magnitude of the imaginary part of $\bar{\omega}$ increases after it becomes negative. The imaginary parts of $\bar{\omega}$ for laminates 1–4 are plotted in Figs. 4–7 which show that severe flutter does not always set in at the values of $\bar{\lambda}_{cr}$ given in these figures. Another approach of judging whether the instability is severe or not is to use the concept of amplitude ratio A_R or logarithmic increment[19, 34]. The amplitude ratio A_R is defined as the increase in amplitude in one cycle, which is equal to $e^{2\pi\omega_I/\omega_R}$ and the logarithmic increment is $\log_e A_R$. $\text{Log}_e A_R$ is plotted against $\bar{\lambda}$ for laminate 3 in Fig. 8, which shows that beyond $\bar{\lambda}_{cr}$ the amplitude does not increase too rapidly with $\bar{\lambda}$. The values of $\bar{\lambda}$ near which amplitudes are expected to increase rapidly are higher than $\bar{\lambda}_{cr}$ and should be close to, but less than, the critical flutter parameter for no damping. These observations are in agreement with those in [34]. Figure 8 also shows the effect of environment (moisture-temperature gradient), aerodynamic damping and prestress. Moisture-temperature gradient appears to stabilize the system. It has also been pointed out earlier that structural damping effects are less when moisture-temperature gradient is present in the laminate, which is a consequence of the master curve for epoxy used in calculations. The stabilization effect is caused by (1) reduced

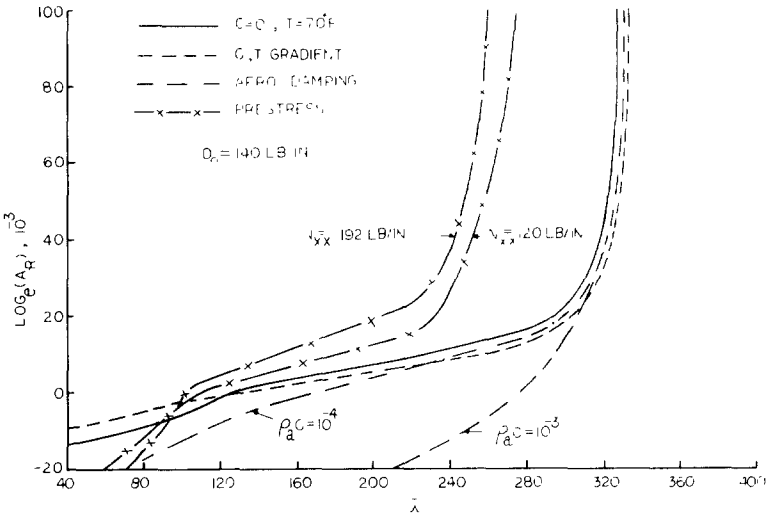

Fig. 8. Effect of environment, aerodynamic damping and prestress on amplitude ratio vs $\bar{\lambda}$ for $(\pm 45/0_2/90)_s$ laminate 3, $a/h = 40$, $h = 0.06$ in

structural damping and (2) increased shear stiffness, but the increase in $\bar{\lambda}_{cr}$ is entirely due to increase in shear stiffness.

Figure 8 also illustrates that $\bar{\lambda}_{cr}$ ($\bar{\lambda}$ at $\log_e A_R = 0$) is significantly increased by the introduction of aerodynamic damping but the amplitude ratio versus $\bar{\lambda}$ plot does not differ significantly from the one with no aerodynamic damping for high values of A_R. The stabilization effects of aerodynamic damping have been observed in other studies[19]. Effects of prestress have been studied for two values of the ratio of prestress to static buckling load, namely 0.5 and 0.8. $\bar{\lambda}_{cr}$ is not significantly altered due to the presence of prestress, but severe flutter sets in at loads lower than that with no prestress. Effects of environment, prestress, and aerodynamic damping on $\bar{\lambda}_{cr}$ are given in Table 2.

Table 2. Effects of environment, aerodynamic damping and prestress on $\bar{\lambda}_{cr}$ for laminate 3

	$\bar{\lambda}_{cr}$
Reference state	125
Moisture-temperature gradient	148
Aerodynamic damping $\rho_a c = 10^{-4}$ lb-sec/in^3	176
Aerodynamic damping $\rho_a c = 10^{-3}$ lb-sec/in^3	280
Prestress $N^0_{xx} = 120$ lb/in. $\approx 0.5 \times$ (static buckling load)	108
Prestress $N^0_{xx} = 192$ lb/in. $\approx 0.8 \times$ (static buckling load)	101

4.7 *Summary of results and general observations*

The following important observations can be made from the results presented.

1. Small material damping lowers the flutter load from the value in the undamped case. The reduction is very significant when shear deformation effects are small or span-to-depth ratio of the panel is large. For small span-to-depth ratios, this reduction is not that significant. In general, higher damping increases the flutter load. Shear deformation effects have strong influence on analytical estimates of flutter characteristics of a laminate.

2. When material damping is present, instability is not always severe at points of incipient flutter. Values of $\bar{\lambda}$ where instability is severe are usually close to $\bar{\lambda}_{cr}$ for no damping.

3. For the type of master curve and shift hypothesis used in this study, moisture-temperature gradient in a laminate may increase the value of $\bar{\lambda}_{cr}$ as well as $\bar{\lambda}$ for a prescribed amplitude ratio A_R. However, the results are strongly dependent on the type of master curve and shift characteristics of the constituents.

4. Aerodynamic damping stabilizes the system and a significant increase is noticed in the critical value of $\bar{\lambda}_{cr}$ as the damping is increased. Prestress destabilizes the system but the effect on $\bar{\lambda}_{cr}$ is not pronounced for values of prestress less than the static buckling load.

5. Bending-extension coupling effects introduced due to the presence of moisture-temperature gradient do not have any significant influence on the flutter characteristics of symmetric laminates.

Acknowledgements—The authors wish to express their sincere appreciation to Drs. Zvi Hashin and B. Walter Rosen for helpful suggestions and comments during various stages of this work.

REFERENCES

1. J. M. Whitney and N. J. Pagano, Shear deformation in heterogeneous anisotropic plates. *J. Appl. Mech.* **37**, 1031 (1970); P. C. Yang, C. H. Norris and Y. Stavsky, Elastic wave propagation in heterogeneous plates. *Int. J. Solids Structures* **2**, 665 (1966).
2. S. B. Dong, Studies relating to the structural dynamic behavior of laminated plates and shells. UCLA-ENG-7236 (1972).
3. S. V. Kulkarni and N. J. Pagano, Dynamic characteristics of composite laminates. *J. Sound Vibrat.* **23**, 127 (1972).
4. C. T. Sun, Theory of laminated plates. *J. Appl. Mech.* **38**, 231 (1971).
5. Z. Hashin, Theory of fiber reinforced materials, NASA CR-1974 (1972).
6. C. W. Bert and S. Chang, In-plane, flexural, twisting and thickness-shear coefficients for stiffness and damping of a monolayer filamentary composite, Final Report (Part I), NASA Grant NGR-37-003-055, School of Aerospace, Mechanical and Nuclear Engineering, Univ. of Oklahoma, Norman, Oklahoma (1972).
7. C. W. Bert and C. C. Siu, Vibration and damping of laminated, composite-material plates including thickness shear effects, Final Report (Part II), NASA Grant NGR-37-003-055, School of Aerospace, Mechanical and Nuclear Engineering, Univ. of Oklahoma, Norman, Oklahoma (1972).
8. R. F. Gibson and R. Plunkett, Dynamic mechanical behavior of fiber-reinforced composites: measurement and analysis. *J. Comp. Mat.* **10**, 325 (1976).
9. A. B Schultz and S. W. Tsai, Dynamic moduli and damping ratios in fiber-reinforced composites. *J. Comp. Mat.* **2**, 368 (1968).
10. R. R. Clary, Vibration characteristics of unidirectional filamentary composite material panels. *ASTM STP* **497**, 415 (1972).
11. A. B. Schultz and S. W. Tsai, Measurements of complex dynamic moduli of laminated fiber-reinforced composites. *J. Comp. Mat.* **3**, 434 (1969).
12. J. R. Vinson, R. B. Pipes, W. J. Walker and D. R. Ulrich (Ed.), The effects of relative humidity and elevated temperature on composite structures, AFOSR TR-77-0030, Center for Composite Materials, University of Delaware (1976).
13. Anon., Advanced composites design guide, Air Force Materials Laboratory, 3rd Edition (2nd Revision) (1976).
14. R. A. Heller *et al.*, Temperature dependence of the complex modulus for fiber-reinforced materials. *ASTM STP* **580**, 298 (1975).
15. D. Roylance and M. Roylance, Influence of outdoor weathering on dynamic mechanical properties of glass/epoxy laminate. *ASTM STP* **602**, 85 (1976).
16. H. Ashley, Aeroelasticity. *Appl. Mech. Rev.* **23**, 119 (1970).
17. E. H. Dowell, Panel flutter: A review of the aeroelastic stability of plates and shells. *AIAA J.* **8**, 385 (1970); E. H. Dowell, *Aeroelasticity of Plates and Shells*. Noordhoff, Leyden (1975).
18. J. M. Hedgepeth, Flutter of rectangular simply supported panels at high supersonic speeds. *J. Aero. Sci.* **24**, 563 (1957)
19. J. Dugundji, Theoretical considerations of panel flutter at high supersonic Mach numbers. *AIAA J.* **4**, 1257 (1966).
20. C. P. Shore, Effects of structural damping on flutter of stressed panels, NASA TN D-4990 (1969).
21. J. A. McElman, Flutter of curved and flat sandwich panels subjected to supersonic flow, NASA TN D-2192 (1964).
22. L. L. Erickson, Supersonic flutter of sandwich panels: effects of face sheet bending stiffness, rotary inertia, and orthotropic core shear stiffness, NASA TN D-6427 (1971).
23. A. A. Permutter, On the aeroelastic stability of orthotropic panels in supersonic flow. *J. Aero. Sci.* **29**, 1332 (1962).
24. R. L. Ramkumar and T. A. Weisshar, Flutter of flat rectangular anisotropic plates in high Mach number supersonic flow. *J. Sound Vibrat.* **50**, 587 (1977).
25. J. W. Sawyer, Flutter of laminated plates in supersonic flow, NASA TM X-72800 (1975).
26. Z. Hashin and B. W. Rosen, The elastic moduli of fiber-reinforced materials. *J. Appl. Mech.* **31**, 233 (1964); Errata **32**, 219 (1965); B. W. Rosen, Thermomechanical properties of fibrous composites. *Proc. R. Soc. Lond. (A)* **319**, 79 (1970).
27. J. C. Halpin and S. W. Tsai, Environmental factors in composite materials design, AFML TR 67-423 (1967).
28. B. W. Rosen, Stiffness of fiber composite materials. *Comp.* (1973).
29. P. C. Chou and J. Carleone, Transverse shear in laminated plate theories. *AIAA J.* **11**, 1333 (1973).
30. S. N. Chatterjee and S. V. Kulkarni, Shear correction factors for laminated plates. *AIAA J.* (in press).
31. S. Mukherjee and E. H. Lee, Study of wave propagation in laminated viscoelastic composites by variational methods. *Proc. 5th Canadian Cong. of Applied Mechanics*, Fredericton (1975).
32. D. H. Kaelble, Dynamic and tensile properties of epoxy resins. *J. Appl. Polymer Sci.* **9**, 1213 (1965).
33. J. C. Halpin, *Introduction to Viscoelasticity, Composite Materials Workshop* (Edited by S. W. Tsai, J C. Halpin and N. J. Pagano). Technomic, New York (1968).
34. G. Herrmann and I C. Jong, On the destabilizing effect of damping in nonconservative elastic systems. *J. Appl. Mech.* **33**, 592 (1965).